

# Flavor Stability Analysis of Supernova Neutrino Fluxes Compared with Simulations

*Srdjan Sarikas<sup>1,2,3</sup>, Georg G. Raffelt<sup>3</sup>*

<sup>1</sup>Dipartimento di Scienze Fisiche, Università di Napoli “Federico II”, 80126 Napoli, Italy

<sup>2</sup>Istituto Nazionale di Fisica Nucleare — Sezione di Napoli, 80126 Napoli, Italy

<sup>3</sup>Max-Planck-Institut für Physik, Föhringer Ring 6, 80805 München, Germany

We apply a linearized stability analysis to simplified models of accretion-phase neutrino fluxes streaming from a supernova. We compare the results with recent numerical studies and find excellent agreement. This provides confidence that a linearized stability analysis can be further applied to more realistic models.

## 1 Introduction

Neutrino-neutrino interactions cause the neutrino flux evolution close to a supernova (SN) core to be nonlinear and numerically very challenging [1]. The flavor instability causing collective flavor conversions can be suppressed by the “multi-angle matter effect” [2]. This point was recently investigated numerically for an accretion-phase model where the matter density near the neutrino sphere is large, using a schematic description of the neutrino fluxes [3]. On the other hand, the flavor stability can also be investigated with a linearized stability analysis, avoiding an explicit solution of the equations of motion [4]. We apply this method to the models of Ref. [3] and find excellent agreement of the stable regime identified with either method.

## 2 Linearized stability analysis

We describe the neutrino flavor evolution in terms of matrices  $\Phi_{E,u,r}$  where the diagonal elements are the usual total number fluxes and the off-diagonal elements encode phase information [2, 5]. We label the angular dependence with  $u$ , in close relation with the neutrino emission angle  $\vartheta_R$  at the inner boundary radius  $R$ ,  $u = \sin^2 \vartheta_R = (1 - \cos^2 \vartheta_r) r^2 / R^2$ . For semi-isotropic emission at a “neutrino sphere” with radius  $R$ , the flux is uniformly distributed on  $0 \leq u \leq 1$ . The equations of motion are  $i\partial_r \Phi_{E,u,r} = [H_{E,u,r}, \Phi_{E,u,r}]$ , with the Hamiltonian [4]

$$H_{E,u,r} = \left( \frac{M^2}{2E} + \sqrt{2} G_F N_\ell \right) \frac{1}{v_{u,r}} + \frac{\sqrt{2} G_F}{4\pi r^2} \int_0^1 du' \int_{-\infty}^{+\infty} dE' \left( \frac{1}{v_{u,r} v_{u',r}} - 1 \right) \Phi_{E',u',r},$$

where  $M^2$  is the neutrino mass-squared matrix,  $N_\ell$  the matrix of net charged-lepton densities which in the flavor basis is  $N_\ell = \text{diag}(n_e - n_{\bar{e}}, n_\mu - n_{\bar{\mu}}, n_\tau - n_{\bar{\tau}})$  and  $v_{u,r}$  is the radial projection of neutrino velocity at the radius  $r$ . Antineutrinos are represented through negative-energy modes ( $E < 0$ ) and negative negative fluxes in the matrices  $\Phi_{E,u,r}$ . This sign convention simplifies the formalism and obviates any distinction between neutrinos and antineutrinos.

Henceforth we drop the explicit subscript  $r$  to denote the  $r$ -dependence of all quantities. In the two flavor scenario one can write:

$$\Phi_{E,u} = \frac{\text{Tr } \Phi_{E,u}}{2} + \frac{F_{E,u,R}^e - F_{E,u,R}^x}{2} S_{E,u} ,$$

where  $F_{E,u}^{e,x}$  are the differential neutrino fluxes at the inner boundary radius  $R$  for the  $e$  and  $x$  flavors. The flux summed over all flavors,  $\text{Tr } \Phi_{E,u}$ , drops out of the equations of motion and is conserved in our free-streaming limit. The “swapping matrix”

$$S_{E,u} = \begin{pmatrix} s_{E,u} & S_{E,u} \\ S_{E,u}^* & -s_{E,u} \end{pmatrix} ,$$

encodes the flavor evolution with initial conditions  $s = 1$  and  $S = 0$ .

We expand the Hamiltonian for large distances from the core and small mixing angle. After dropping its trace we find

$$\begin{aligned} H_{E,u}^{\text{vac}} &= \frac{M^2}{2E} v_u^{-1} \rightarrow \pm \frac{\omega}{2} \begin{pmatrix} \cos 2\theta & \sin 2\theta \\ \sin 2\theta & -\cos 2\theta \end{pmatrix} v_u^{-1} \rightarrow \pm \frac{\omega}{2} \begin{pmatrix} 1 & 0 \\ 0 & -1 \end{pmatrix} \left(1 + \frac{u}{2} \frac{R^2}{r^2}\right) , \\ H_{E,u}^{\text{m}} &= \sqrt{2} G_F \begin{pmatrix} n_e - n_{\bar{e}} & 0 \\ 0 & 0 \end{pmatrix} v_u^{-1} \rightarrow \frac{\tilde{\lambda}}{2} \begin{pmatrix} 1 & 0 \\ 0 & -1 \end{pmatrix} \left(1 + \frac{u}{2} \frac{R^2}{r^2}\right) , \\ H_{E,u}^{\nu\nu} &\rightarrow \frac{\sqrt{2} G_F R^2}{4\pi r^4} \int_0^1 du' \frac{u+u'}{2} \int_{-\infty}^{+\infty} dE' \frac{F_{E,u,R}^e - F_{E,u,R}^x}{2} S_{E',u'} . \end{aligned}$$

where  $\tilde{\lambda} = \sqrt{2} G_F (n_e - n_{\bar{e}})$ . We write the neutrino-neutrino part concisely in the form  $H_{E,u}^{\nu\nu} \equiv \mu_r \int_0^1 du' \frac{1}{2} (u+u') \int_{-\infty}^{+\infty} dE' g_{E,u} S_{E',u'}$ , where  $\mu_r = \mu_R R^4 / 2r^4$  encodes the strength of the neutrino-neutrino interaction with the parameter  $\mu_R = \sqrt{2} G_F (F_R^{\bar{\nu}e} - F_R^{\nu x}) / 4\pi R^4$ . We further define the dimensionless flavor difference spectrum  $g_{E,u} = (F_{E,u,R}^e - F_{E,u,R}^x) / (F_R^{\bar{\nu}e} - F_R^{\nu x})$  with the normalization in the antineutrino sector  $\int_{-\infty}^0 dE \int_0^1 du g_{E,u} = -1$ . The integration over neutrinos (positive energies) gives  $\int_0^\infty dE \int_0^1 du g_{E,u} = (F_R^{\nu e} - F_R^{\nu x}) / (F_R^{\bar{\nu}e} - F_R^{\nu x}) \equiv 1 + \varepsilon$ , with  $\varepsilon$  being asymmetry of the spectra.

Next we expand the equations in the small-amplitude limit  $|S| \ll 1$  which implies, to linear order,  $s = 1$ . After switching to the variable  $\omega = \Delta m^2 / 2E$  for the energy modes one finds [4]

$$i\partial_r S_{\omega,u} = [\omega + u(\lambda + \varepsilon\mu)] S_{\omega,u} - \mu \int du' d\omega' (u+u') g_{\omega'u'} S_{\omega',u'} .$$

Here  $\lambda = \tilde{\lambda} R^2 / 2r^2$  encodes the imprint of multi-angle matter effect. Except for the additional two powers of  $r^{-1}$  this quantity describes the SN density profile and scales approximately as  $\mu_r \propto r^{-4}$ .

Writing solutions of the linear differential equation in the form  $S_{\omega,u} = Q_{\omega,u} e^{-i\Omega r}$  with complex frequency  $\Omega = \gamma + i\kappa$  and eigenvector  $Q_{\omega,u}$  leads to the eigenvalue equation [4],

$$(\omega + u\bar{\lambda} - \Omega) Q_{\omega,u} = \mu \int du' d\omega' (u+u') g_{\omega'u'} Q_{\omega',u'} ,$$

where  $\bar{\lambda} \equiv \lambda + \varepsilon\mu$ . The solution has to be of the form  $Q_{\omega,u} = (A + Bu) / (\omega + u\bar{\lambda} - \Omega)$ . Solutions exist if  $\mu^{-1} = I_1 \pm \sqrt{I_0 I_2}$ , where  $I_n = \int d\omega du g_{\omega,u} u^n / (\omega + u\bar{\lambda} - \Omega)$ . The system is stable if all  $\Omega$  are purely real. A possible imaginary part,  $\kappa$ , is the exponential growth rate.

### 3 Results

We aim at comparing the linearized stability analysis with the numerical solutions of Ref. [3] who numerically solved the neutrino flavor evolution for a  $10.8 M_\odot$  model at various post bounce times. They confirmed the multi-angle matter suppression of self-induced flavor conversion, but also found partial conversions at a large radius for the models  $200 \text{ ms} \lesssim t_{\text{pb}} \lesssim 300 \text{ ms}$ .

We use the same schematic half-isotropic and monochromatic spectra, leading to the simple form  $g_{\omega,u} = -\delta(\omega + \omega_0) + (1 + \varepsilon) \delta(\omega - \omega_0)$ . The integrals  $I_n$  can now be evaluated analytically. Then it is easy to find a solution  $(\gamma, \kappa)$  for each pair  $(\mu, \lambda)$ . Figure 1 shows the region where  $\kappa \neq 0$  for two snapshots together with the  $\kappa$  isocontours. We also show the “SN trajectory” in the  $(\mu, \lambda)$  plane, i.e. essentially the density profile as a function of radius because  $\mu_r \propto r^{-4}$ .

Our results agree with the numerical solutions of Ref. [3] for all models. Whenever the numerical solutions find no flavor conversion, our SN trajectory indeed stays clear of the unstable regime. Conversely, when it briefly enters the unstable regime as in the left panel of Fig. 1, we reproduce the onset radius for partial flavor conversion of Ref. [3]. The linear stability analysis correctly explains the numerical results.

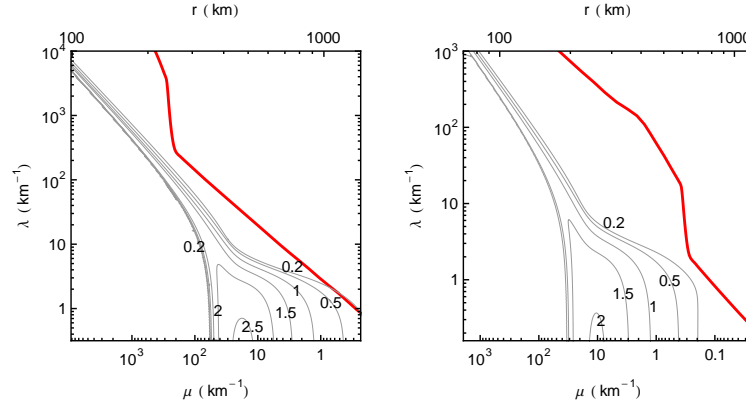


Figure 1: Contours of  $\kappa$  and the trajectory of SN (thick red line) at  $t = 300 \text{ ms}$  (left) and  $400 \text{ ms}$  (right) post bounce for a  $10.8 M_\odot$  model discussed in Ref. [3].

It is interesting that in principle the SN trajectory can enter the instability region twice. As a toy model we consider the density profile  $\lambda \sim 0.43 \mu$  with half-isotropic emission at  $R = 10 \text{ km}$  and  $\mu_r = 7 \times 10^4 \text{ km}^{-1} R^4 / 2r^4$ . In Fig. 2 we show  $\kappa(r)$  and the evolution of the off-diagonal element  $|S|$ . Indeed  $|S|$  oscillates and grows in the unstable regime, only oscillates when  $\kappa = 0$ , and then grows again during the second instability crossing. It remains to be seen if there are realistic density profiles where such a multiple instability situation exists in practice.

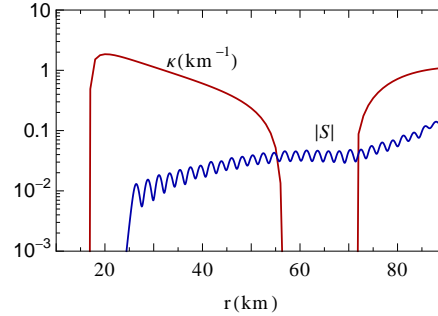


Figure 2: Growth rate  $\kappa$  and off-diagonal element  $|S|$  for a toy model (see text).

## 4 Conclusions

The nonlinear neutrino flavor evolution in the SN environment can be a challenging numerical task even when it only consists of post-processing the output of a self-consistent SN simulation, not to mention solving self-consistently the multi-flavor neutrino transport. The latter is not necessary if collective oscillations do not happen in the critical region below the shock wave. The question if a given SN model with concomitant neutrino fluxes is stable against self-induced flavor conversion can be answered with a linearized stability analysis [4]. Of course, if the model is unstable, one needs to solve the equations numerically to find the final outcome. However, since neutrino fluxes during the accretion phase may well be stable because of the multi-angle matter effect, a linearized flavor stability analysis is here a useful tool.

We have applied this method to the models studied in Ref. [3] and compared with the outcome of their numerical solutions. The results are very encouraging in that we can perfectly account for the results of the numerical simulations and can also predict the onset radius for those cases where partial flavor conversion occurs at a large radius.

Meanwhile we have applied this method to an accretion-phase model with realistic energy and angle distributions [5]. We find that a stability diagram in the form of our Fig. 1 is an excellent tool to summarize the flavor stability situation of SN neutrino fluxes.

## 5 Acknowledgments

We thank Sovan Chakraborty and collaborators for providing us their SN models and Irene Tamborra and Javier Redondo for comments on the manuscript. We also thank the organizers of the HANSE 2011 workshop for a very informative meeting and the opportunity to present our results on very short notice. Partial support by the Deutsche Forschungsgemeinschaft under grants TR 27 and EXC 153 is acknowledged.

## References

- [1] H. Duan, G. M. Fuller and Y.-Z. Qian, “Collective neutrino oscillations,” *Ann. Rev. Nucl. Part. Sci.* **60** (2010) 569.
- [2] A. Esteban-Pretel, A. Mirizzi, S. Pastor, R. Tomàs, G. G. Raffelt, P. D. Serpico and G. Sigl, “Role of dense matter in collective supernova neutrino transformations,” *Phys. Rev. D* **78** (2008) 085012.
- [3] S. Chakraborty, T. Fischer, A. Mirizzi, N. Saviano and R. Tomàs, “Analysis of matter suppression in collective neutrino oscillations during the supernova accretion phase,” *Phys. Rev. D* **84** (2011) 025002.
- [4] A. Banerjee, A. Dighe and G. G. Raffelt, “Linearized flavor-stability analysis of dense neutrino streams,” *Phys. Rev. D* **84** (2011) 053013.
- [5] S. Sarikas, G. G. Raffelt, L. Hüpohl and H.-T. Janka, “Flavor stability of a realistic accretion-phase supernova neutrino flux,” *arXiv:1109.3601*.